Environmental Research Letters

LETTER

Renewable-powered desalination as an optimisation pathway for renewable energy systems: the case of Australia's Murray–Darling Basin

Michael Heihsel[1,4], **Syed Muhammad Hassan Ali**[2], **Julian Kirchherr**[3] **and Manfred Lenzen**[2]

[1] Department of Energy Engineering, Technical University of Berlin, Berlin, Germany
[2] ISA, School of Physics, The University of Sydney, Sydney, New South Wales 2006, Australia
[3] Copernicus Institute of Sustainable Development, Utrecht University, Utrecht, The Netherlands
[4] Author to whom any any correspondence should be addressed.

E-mail: michael.heihsel@campus.tu-berlin.de

Keywords: renewable energy, desalination, climate change, load-shifting, water management

Supplementary material for this article is available online

OPEN ACCESS

RECEIVED
1 August 2019

REVISED
7 October 2019

ACCEPTED FOR PUBLICATION
14 November 2019

PUBLISHED
11 December 2019

Abstract

The ecology in the Murray–Darling Basin in Australia is threatened by water scarcity due to climate change and the over-extraction and over-use of natural water resources. Ensuring environmental flows and sustainable water resources management is urgently needed. Seawater desalination offers high potential to deliver water in virtually unlimited quantity. However, this technology is energy-intensive. In order to prevent desalination becoming a driver of greenhouse gases, the operation of seawater desalination with renewables is increasingly being considered. Our study examines the optimisation of the operation of a 100% renewable energy grid by integrating seawater desalination plants and pipelines as a variable load. We use a GIS-based renewable energy load-shifting model and show how both technologies create synergy effects. First, we analyse what quantity of water is missing in the basin in the long run. We determine locations for seawater desalination plants and pipelines to distribute the water into existing storages in the Murray–Darling Basin. Second, we design a pipeline system and calculate the electricity needed to pump the water from the plants to the storages. Third, we use the combined renewable energy load-shifting model. We minimise the total cost of the energy system by shifting energy demand for water production to periods of high renewable energy availability. Our calculations show that in such a system, the unused spilt electricity can be reduced by at least 27 TWh. The electricity system's installed capacity and levelised cost of electricity can be reduced by up to 29%, and 43% respectively. This approach can provide an annual net economic benefit of $22.5 bn. The results illustrate that the expansion of seawater desalination capacity for load-shifting is economically beneficial.

Abbreviations

GIS	Geographic information system
LCOE	Levelised cost of electricity
MDB	Murray–Darling Basin
MDBA	Murray–Darling Basin Authority
RE	Renewable energies
RO	Reverse osmosis
SDL	Surface-water diversion limit
SWRO	Seawater reverse osmosis

1. Introduction

The Murray–Darling Basin (MDB) is Australia's largest river catchment. The MDB includes about

30 000 wetlands and the multinational Ramsar Convention on Wetlands protects 16 of these wetlands (Forghani *et al* 2011). Between 1997 and 2009, Australia and especially the MDB suffered heavily from drought (Leblanc *et al* 2012). The MDB supplies about 20 million people with food (Forghani *et al* 2011), and Agricultural production in the MDB amounts to $24 bn (Murray–Darling Basin Authority 2019a). The natural habitat of many animal and plant species, and the agricultural economy are in danger (Crimp *et al* 2010) (Kirby *et al* 2014) (Kirby *et al* 2012) (Wittwer and Griffith 2011). Extreme and changeable climate conditions have intensified recently. Following the hottest December since records began, January 2019 marked the hottest month ever measured (Bureau of Meteorology 2019).

To fight the drought in the MDB, the Australian government passed the Water Act 2007 (The Parliament of Australia 2007). Based on this, the Murray–Darling Basin Authority (MDBA) published the Guide to the Proposed Basin Plan in 2010 (Murray–Darling Basin Authority 2010). In it, the MDBA stated that it plans to shorten the existing water allocation rights and thereby to increase natural flows (Connell and Grafton 2011). In a recently published study, Williams and Grafton (2019) have shown that the government's actions worth $3.5 bn to increase water flows in the MDB are failing.

Desalination has a high technical potential to provide large amounts of additional water. Since the millennium drought, every major city in Australia operates a seawater desalination plant (El Saliby *et al* 2009). Porter *et al* (2015) have shown that desalination can be a strategy for the economic development of arid coastal regions. Reverse osmosis (RO) is the leading desalination technology worldwide. With 3–5 kWh m^{-3}, RO is more energy-efficient than other thermal desalination technologies, which results in lower specific costs of less than $0.75 per m^3 (Bennett 2011) (Alhaj and Al-Ghamdi 2019a). Nevertheless, RO is an energy-, and therefore carbon-intensive technology when operated with conventional energy. When operated within the Australian grid, electricity causes over 90% of carbon emissions during operation (Heihsel *et al* 2019). Renewable energy (RE) thus solves a fundamental issue with desalination, rendering the process sustainable (The World Bank 2012) (Baten and Stummeyer 2013) (Ghaffour *et al* 2014). Despite its high ecological potential, only 1% of desalination water worldwide is produced using RE (Shahzad *et al* 2017). Market barriers for widespread use are high capital costs and uncertainty over optimal system integration strategies (Alhaj and Al-Ghamdi 2019b). A high proportion of RE in the electricity grid requires a completely different operational management (Olatomiwa *et al* 2016). Australia has a high potential for generating electricity from renewable resources. However, without corresponding operational management, the generation capacity is about three times larger than the current capacity in an almost exclusively conventional energy system (Lenzen *et al* 2016). Seawater desalination can buffer the volatility in renewable electricity production, which in turn is followed by economic benefits due to the reduction in generation capacity.

Some researchers and operators believe that RO should be operated in a steady state. However, membrane technology has evolved significantly in recent years. As a result, more flexible operation in a partial load range is possible without damaging membranes (Ghobeity and Mitsos 2010). Although the durability of the membranes will be reduced by intermittent operation, operating with antiscalant and rinsing reduces this effect significantly (Freire-Gormaly and Bilton 2018). Anyway, with 32%, electricity contributes significantly to the total cost of water production, while membranes account for just 4% of the total costs and they are becoming continually cheaper (the other cost components are 38% capital costs, 13% labour costs, 9% chemicals, and 4% other parts) (Ziolkowska 2015). To realise a flexible operation, desalination plants can be provided by a positive displacement pump with a variable frequency drive (Ghobeity and Mitsos 2010). Numerous studies show the feasibility of RO's direct operation with intermittent energies such as wind and sun (Li *et al* 2019) (Richards *et al* 2014) (Bognar *et al* 2013) (Richards *et al* 2011) (Park *et al* 2012) (Park *et al* 2011). Besides, practical examples show the feasibility of direct coupling of RO and RE and the associated variability of electricity (Desalination.biz 2017) (Augsten 2007).

For the first time, our study examines the economic benefits of coupling a large seawater desalination and pipeline system with a 100% RE grid within a Geographic Information System (GIS) based load-shifting model. At the same time, we introduce an entirely new approach to the water management of a large basin like the MDB. In doing so, we address a crucial problem of arid regions in the critical area of the water-energy-food nexus (Leck *et al* 2015) (Scanlon *et al* 2013) (Grubert and Webber 2015). This study is particularly relevant for water management and energy practitioners, such as government agencies and engineers. Furthermore, our study shows the potential for additional benefit from the coupling of both technologies. Policymakers can benefit from this knowledge regarding the implementation of regulatory frameworks.

2. Methods and data

2.1. A 100% renewable energy model[5]

We used a GIS-based electricity dispatch model with a geographic resolution of 90 × 110 grid boxes by Lenzen *et al* (2016). Within this model, we simulated a

[5] Please see supplementary material S1 for more details.

sequential competitive bidding process that proceeds hourly over one year. In our dispatch optimisation model of the RE system, we simulated a spot market with competitive bidding. We optimised the cost of power generation sequentially and iteratively for every hour and every location. The algorithm proceeds by the following steps:

1. The generators supply the demand for every hour and every location grid box of the optimisation period. We rank all generators according to the lowest total cost for each hour and location separately. The total cost results from variable cost and fixed cost per MWh. Variable costs and fuel costs are data-based. We estimate fixed capital, maintenance and transmission costs for the first run.
2. After a run, the model recalculates the pre-run estimated fixed costs with the endogenously determined capacity factor. Based on these post-run costs, the algorithm calculates the total cost for each generator.
3. The algorithm adjusts the transmission network according to the new generator capacity and location.
4. We rank all generators based on cost efficiency over the entire optimisation period. We subsequently exclude inefficient generators.
5. The algorithm repeats the exclusion of inefficient generators while the reliability standard of 0.002% of the total demand complies.

Lenzen *et al* (2016) have provided a more detailed formal description of the optimisation approach.

2.2. The load-shifting algorithm

Our load-shifting algorithm is based on the work of Ali *et al* (2018), Ali *et al* (2019), and Keck *et al* (2019). Our concept of using the demand of seawater desalination for load-shifting has the following additional key benefits:

- Seawater reverse osmosis plants (SWRO) have a high electricity consumption which is available for load-shifting.
- The plants are utility-scale; in other words, they are centrally and simply controllable. They do not depend directly on a specific user behaviour. Thus, network operators can directly control them.
- Unlike electricity, water can easily and economically be stored in large reservoirs.

We integrated the load-shifting algorithm into the clean grid optimisation model from Lenzen *et al* (2016). We considered the electricity load of Australia as a non-shiftable load. We use the additional load of desalination and pipelines for the load-shifting procedure. The algorithm applies the locally and hourly optimised electricity system from Lenzen's clean grid as a starting point. The algorithm shifts demand from expensive generators to cheaper ones to utilise spilt energy. Spilt energy is the generated electricity which cannot be utilised due to missing demand at a specific time. It runs according to the following procedure:

1. We set a load-shifting period that determines a time range that the algorithm considers for the shifting. For our study, we considered shifting periods of 10 d, 30 d, and 90 d, respectively. The length of the periods is derived from the ability to store water in more extended periods. The computational requirement increases exponentially with the extension of the shifting period.
2. The variables of generated and spilt electricity are ranked separately.
3. The programme consequently shifts the demand within the load-shifting period from the generators with the highest cost to those with the lowest cost that produce spilt electricity. We determine the load-shifting potential $\mathbf{P}$ by

$$\mathbf{P} = \min\left[\mathbf{G}_{\text{inefficient}}(\mathbf{t} + \Delta t_s), \mathbf{S}_{\text{efficient}}(\mathbf{t}), \mathbf{D}(\mathbf{t} + \Delta t_s)\right], \quad (1)$$

   where $\mathbf{G}_{\text{inefficient}}$ is the generation of the expensive generator, which we reduce. $\mathbf{S}_{\text{efficient}}$ is the spilt energy of the cost-efficient generator. $\mathbf{D}$ is the electricity demand of the SWROs that is available for shifting. The variable $\mathbf{t}$ determines each hour of the optimisation period. The period Δt_s is the shifting period. The algorithm considers every single hour within the shifting period.
4. The next step is to update the variables of the power generation to

$$\mathbf{G}^{\text{update}}_{\text{efficient}}(\mathbf{t}) = \mathbf{G}_{\text{efficient}}(\mathbf{t}) + \mathbf{P} \quad (2)$$

   and

$$\mathbf{G}^{\text{update}}_{\text{inefficient}}(\mathbf{t} + \Delta t_s) = \mathbf{G}_{\text{inefficient}}(\mathbf{t} + \Delta t_s) - \mathbf{P}. \quad (3)$$

   $\mathbf{G}_{\text{efficient}}$ is the electricity produced by the cost-efficient generators. $\mathbf{G}_{\text{inefficient}}$ is the electricity produced by reduced inefficient generators. The index update marks the adjusted variables.
5. As with the variables of electricity generation, we update the spilt energy variables resulting in

$$\mathbf{S}^{\text{update}}_{\text{efficient}}(\mathbf{t}) = \mathbf{S}_{\text{efficient}}(\mathbf{t}) - \mathbf{P} \quad (4)$$

   and

$$\mathbf{S}^{\text{update}}_{\text{inefficient}}(\mathbf{t} + \Delta t_s) = \mathbf{S}_{\text{inefficient}}(\mathbf{t} + \Delta t_s) + \mathbf{P}. \quad (5)$$

   Here, $\mathbf{S}_{\text{efficient}}$ is the spilt energy of the efficient generator, which is utilised by the shifted demand. $\mathbf{S}_{\text{inefficient}}$ is the spilt energy of the inefficient

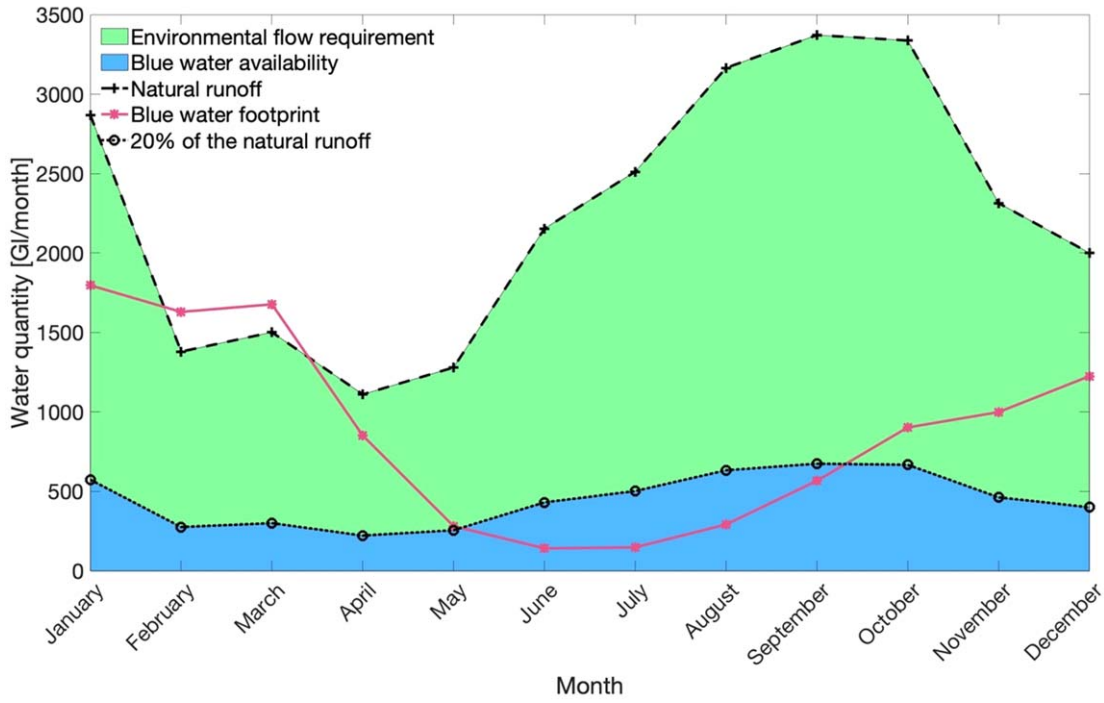

Figure 1. The water availability in the MDB according to (Hoekstra *et al* 2012); own depiction.

generator, which is increased by the shifting. The algorithm aims to supply the demand throughout the optimisation period by efficient generators alone. Consequently, we eliminate inefficient generators from the system.

6. Finally, we update the electricity demand **D** by the shifted reduction potential. We reduce electricity production by the reduction potential at time $(\mathbf{t} + \Delta t)$ and shift it to **t**, which is represented by

$$\mathbf{D}^{\text{update}}(\mathbf{t} + \Delta t_s) = \mathbf{D}(\mathbf{t} + \Delta t_s) - \mathbf{P} \quad (6)$$

and

$$\mathbf{D}^{\text{update}}(\mathbf{t}) = \mathbf{D}(\mathbf{t}) + \mathbf{P}. \quad (7)$$

We repeat from step 3 onwards for every hour and every demand location. The shifting ends when either the available demand **D** is completely shifted or when no more spilt energy is available. After the load-shifting programme has optimised all hours and locations, all inefficient generators that are no longer needed are removed from the system. Subsequently, we adjust the transmission system and the total demand.

2.3. Modelling the desalination energy demand

2.3.1. Total desalination water demand

The government's Guide to the Proposed Basin Plan (Murray–Darling Basin Authority 2010) demanded a total of between 3000 and 7600 Gl per year of recovered water in order to achieve the objectives of the Water Act 2007 (The Parliament of Australia 2007). For economic reasons, the MDBA recommended that no more than 4000 Gl should be recovered. In the end, the government agreed on only 2750 Gl (Murray–Darling Basin Authority (2012)).

Hoekstra *et al* (2012) have calculated the total runoff and the blue water footprint for the MDB, including the resulting available water according to the presumptive environmental standard (see figure 1) (Richter *et al* 2012) (Hoekstra *et al* 2011). During the months where demand exceeds supply, water should be added from outside the system. The water shortage is the difference between blue water availability and the blue water footprint. We calculated the difference for each month and added up all negative water budgets, which results in 6200 Gl. However, it is conceivable that from May to September when the budget is positive, water is stored to compensate for negative budgets in other months. In this way, the water shortage would amount to 5100 Gl. We calculated a weighted average of both values, with a slightly higher weighting of the lower limit (60%) which results in 5500 Gl.

2.3.2. Local water distribution

We estimated locations and capacities of desalination plants that pump the produced water into existing storages via a modelled pipeline system. Therefore, we used 31 MDBA government storages and data concerning their capacity and extended this with coordinates, altitudes and direct distances to the sea (Murray–Darling Basin Authority 2019b). We locally distributed the 5500 Gl of water in the MDB according to the relative demand of the areas. For this purpose, we followed the area delineation according to Murray–Darling Basin Authority (2018) and used the water

demand data for the 29 areas. Pipelines supplied the desalinated water to storages in or near the area. Each storage was supplied by one or more pipelines. Each pipeline, in turn, supplied one or more storages. We have planned 29 sites for pipelines and desalination plants. We considered 35 pipelines, which were determined endogenously. The number of desalination plants has not been determined because only location and capacity are critical for the modelling.

Distributing the water to the pipeline locations required the following steps:

1. In a GIS analysis, we linked all storages to the areas in which they are located. If there was no storage in an area, we allocated the closest storage.

2. The pipelines temporarily supplied the storages with water. From the storages, the water was distributed to the areas. We created a $i \times j$ concordance **C**, which describes the supply links between the pipelines and the areas. The rows represent area *i*; the columns represent pipeline *j*. The concordance consists of ones and zeros. If pipeline *j* supplies water to area *i*, then $c_{ij} = 1$, otherwise $c_{ij} = 0$.

3. We determined the distribution of the water among the areas. For this, we used the data from the surface water diversion limit (SDL) Trial Water Take Account (Murray–Darling Basin Authority 2018). We calculated the average demand **d** of area *i* of the annual Take Account for the years 2012–13–2016–17. With these data, we calculated the percentage distribution **r** of the demand in area *i* by

$$\mathbf{r} = \frac{\mathbf{d}}{\sum_{i=1}^{29} \mathbf{d}}, \tag{8}$$

4. We calculated the capacity fraction **p** of the pipelines *j*,

$$\mathbf{p} = \frac{\mathbf{c}}{\sum_{j=1}^{29} \mathbf{c}}, \tag{9}$$

where the vector **c** is the capacity of the pipelines *j* resulting from the capacity of the supplied storages.

Each area *i* is supplied by one or more pipelines. The sum **s** of the capacity fractions for each area *i* results in

$$\mathbf{s} = \mathbf{C} * \mathbf{p}, \tag{10}$$

where the column vector **s** is the sum of the capacity fractions of the pipelines supplying each area *i*. In the next step, we modified the concordance **C** by placing the capacity fraction **p** of the pipeline *j* where $c_{ij} = 1$. Therefore

$$\tilde{\mathbf{C}} = \mathbf{C} * \hat{\mathbf{p}}, \tag{11}$$

where $\tilde{\mathbf{C}}$ is the modified concordance, and $\hat{}$ denotes the diagonalisation. For each $\tilde{c}_{ij}$, the capacity fraction of pipeline *j* that supplies area *i* was divided by the sum of the capacity fractions of all pipelines supplying area *i*, resulting in

$$\dot{\mathbf{C}} = \hat{\mathbf{s}}^{-1} * \tilde{\mathbf{C}}. \tag{12}$$

For each *i*, $\sum_{j=1}^{29} \dot{c}_{ij} = 1$ applies. So far, the concordance **C** merely indicated that an area receives water from a given pipeline. The normalised concordance $\dot{\mathbf{C}}$ indicates the percentage of water for each area *i* delivered by pipeline *j*.

5. We calculated the amount of water **w** supplied by pipeline *j* by multiplying the transposed normalised concordance $\dot{\mathbf{C}}'$ by the vector **r**, resulting in

$$\mathbf{q} = \dot{\mathbf{C}}' * \mathbf{r}. \tag{13}$$

The vector **q** indicates the percentage distribution of the water on the pipelines *j*. To distribute the total amount of water *l* to the pipelines, we calculated

$$\mathbf{w} = l * \mathbf{q}, \tag{14}$$

where **w** is the vector for the amount of water that each pipeline *j* supplies, and *l* is the total quantity of 5500 Gl of water. Figure 2 shows the MDB with the locations of the storages, the pipelines, the desalination plants, and the areas overlaid.

2.3.3. The electricity demand of the pipeline and desalination locations

We have iteratively optimised the pipelines' diameters based on their hydraulic head loss h_f. The iteration procedure is explained in more detail in the supplementary material S2, which is available online at stacks.iop.org/ERL/14/124054/mmedia. We limited the maximum diameter to 3.1 m[6]. If the diameter exceeded this limit, we added another pipeline to this location and split up the flow. The specific energy consumption *e* for each pipeline results in

$$e = \frac{\rho\, g\, (b + h_f)}{\eta_{\text{tot}} * 3.6 * 10^6}, \tag{15}$$

where ρ represents the density of water, g the gravitational acceleration, *b* the altitude and η_{tot} the total efficiency of the motor and pump, with an assumed $\eta_{\text{tot}} = 0.873$.

2.3.4. Electricity demand profiles

For the desalination plants, we assumed a specific electricity consumption of $e_{\text{desal}} = 3.5 \frac{\text{kWh}}{\text{m}^3}$, which corresponds to the average value for large SWROs (Heihsel *et al* 2019). Thus, we used the vector ***e*** with the specific electricity consumption for all pipelines to calculate the specific electricity demand $\mathbf{e_{spec}}$ for each desalination/pipeline location by

[6] For comparison: the diameter of the Victorian desalination plant pipeline is 1.93 m (Aquasure 2015).

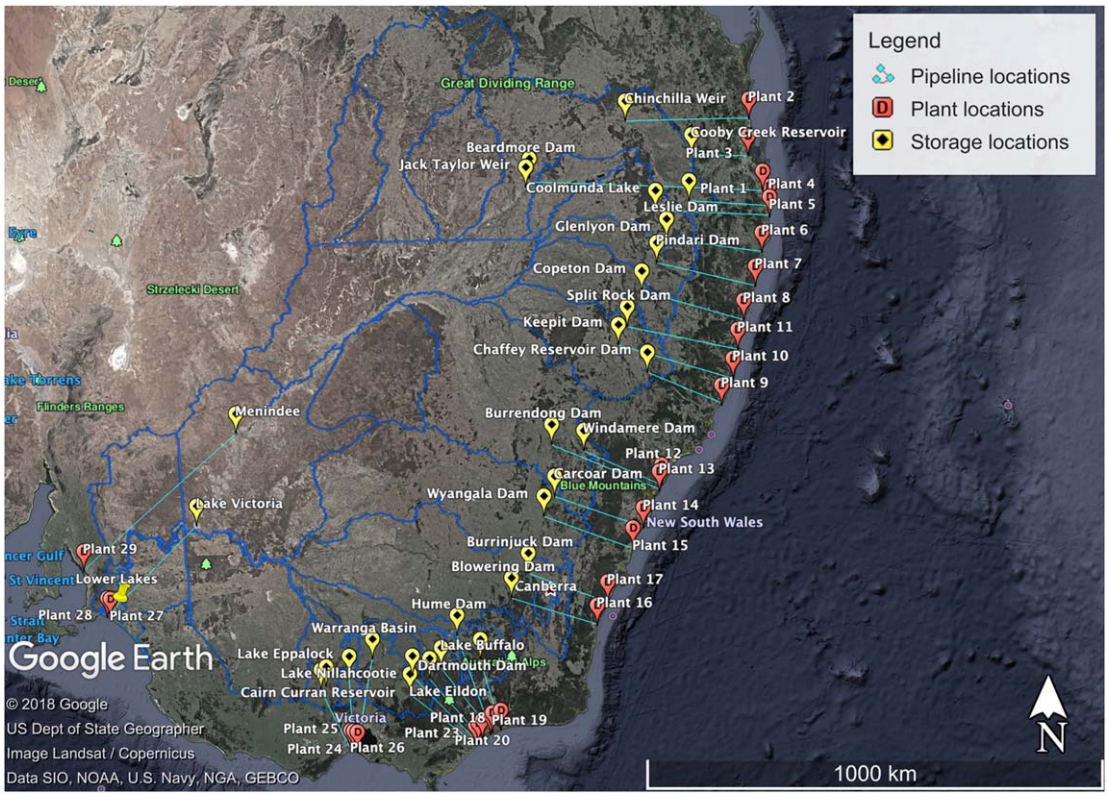

Figure 2. Locations of the storages, the desalination plants, the pipelines and the MDB areas.

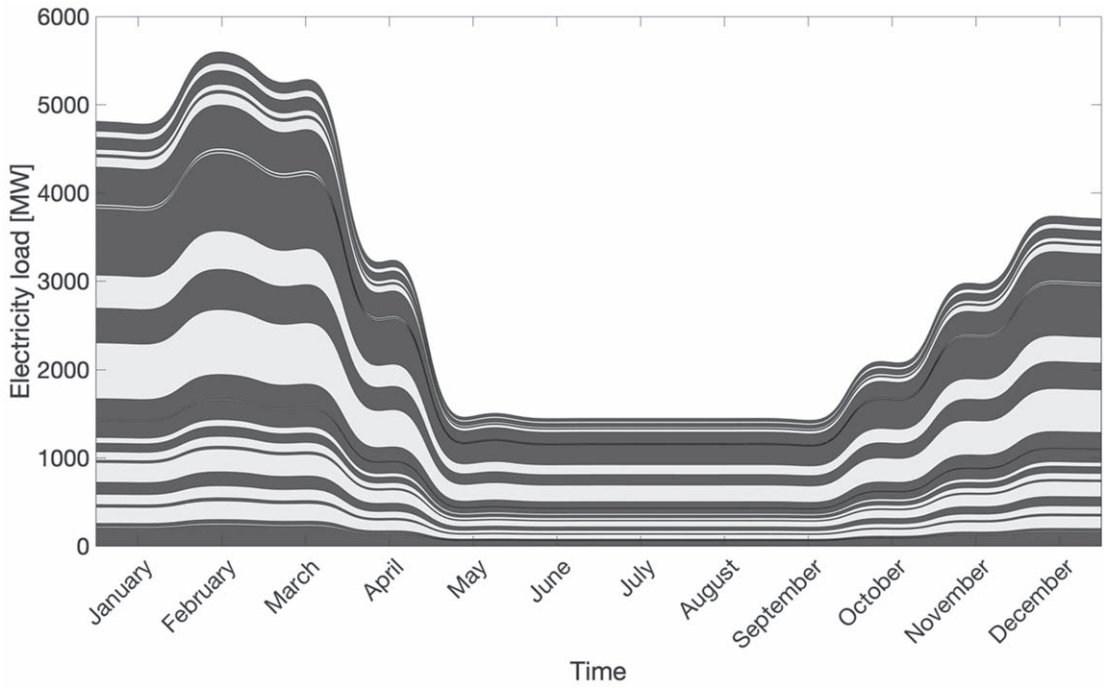

Figure 3. Monthly distributed electricity demand of the 29 combined pipeline and desalination locations.

$$\mathbf{e}_{\text{spec}} = e_{\text{desal}} + \mathbf{e}. \tag{16}$$

$$\mathbf{e}_{\text{tot}} = \mathbf{e}_{\text{spec}} \# \mathbf{w} * 10^{-3}, \tag{17}$$

We get the vector with the total electricity demand $\mathbf{e}_{\text{tot}}$ for all locations by

where $\mathbf{w}$ is the vector with the water demand of all pipelines from equation (14), and # denotes the elementwise multiplication. From monthly profiles of missing water in the MDB (Hoekstra *et al* 2012), we

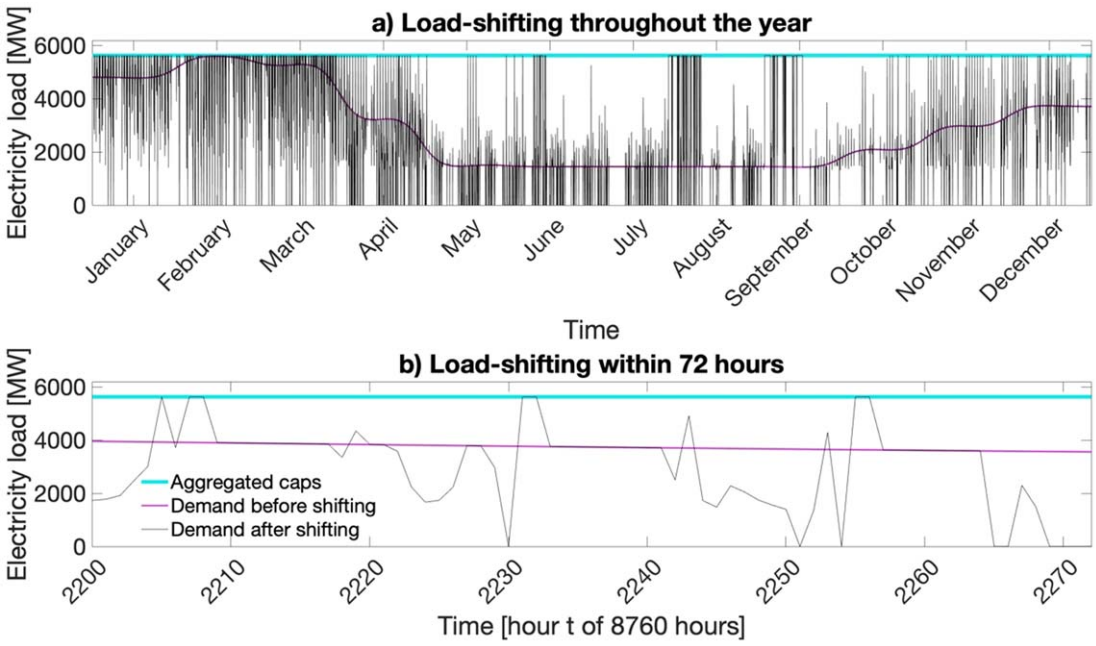

Figure 4. Aggregated electricity demand before and after the load-shifting process for the 10 d load-shifting period. Subplot (a) shows the entire observation period of one year. Subplot (b) shows a period of 72 h.

derived a monthly percentage distribution profile. In order to avoid huge production differences between individual months, we equally distributed a share of the total electricity demand over the year. We distributed 50% of the electricity demand (from equation (17)) as a constant baseload throughout the year, and the remaining 50% was distributed using the monthly percentage distribution profiles. Figure 3 shows the compiled and curve fitted load profiles. Finally, we used the 29 hourly resolved electricity demand profiles for the load-shifting analysis.

3. Results and discussion

3.1. Electricity demand-side implications

Subplot (a) of figure 4 shows the electricity demand of the ten-day load-shifting period scenario.[7] In the load-shifting program, we set demand caps (according to the oversize factor of 1.5) that specify the largest possible electricity demand for the desalination and pipeline spots (blue line). We note that the load-shifting algorithm exploits the maximum values especially in the Australian summer months (October—April). At the same time, the demand available for shifting is exploited to zero more extensively in the winter months.

We also recognise that the months around the Australian summer from October to April ('high-season months') dominate in demand before shifting. As a result of the load-shifting, the 'low-season months' from May to September were used more intensively for desalination. The considerable shifting period is possible in particular due to the large storage capacities in the MDB. The shift in water production from summer to winter thus allows more cost-effective production of water, as we can reduce the capacity of the power generation system.

Subplot (b) shows a typical load variation within 72 h for the 10 d load-shifting period. In our calculation, we did not limit the variability of ramp-ups and shut-downs. We analysed the variability of demand for load-shifting on a daily basis. For the load-shifting with a shifting period of 10 d, the median of the coefficient of variation of all days is 0.33. The largest value is 1.53, the smallest 1×10^{-16}. Although this shows a significant variability in the resulting demand, the variability is realistic for the real operation of seawater desalination plants (Freire-Gormaly and Bilton 2018) (Richards *et al* 2014) (Park *et al* 2012).

In figure 5, we see the monthly average shift by time of day. Positive values show the amount of electricity that was shifted to the specific hour of a month so that desalination plants utilise additional electricity at these points. A negative value shows that demand was reduced in this hour of the month. We recognise the shift in demand from summer to winter, which has already been discussed above, causing a seasonal balance of demand. The axis of hours shows a significant shift to the morning hours until early noon. This effect is strong around April and at the end of the year. Around 5 a.m. and 7 p.m., a systematic reduction of the resulting demand can be observed throughout the year. We explain this effect by the combination of high residual demand and low electricity supply, in particular from solar power. The negative peaks of the

[7] Please see supplementary material S3 for the results of the 30 and 90 d load-shifting periods.

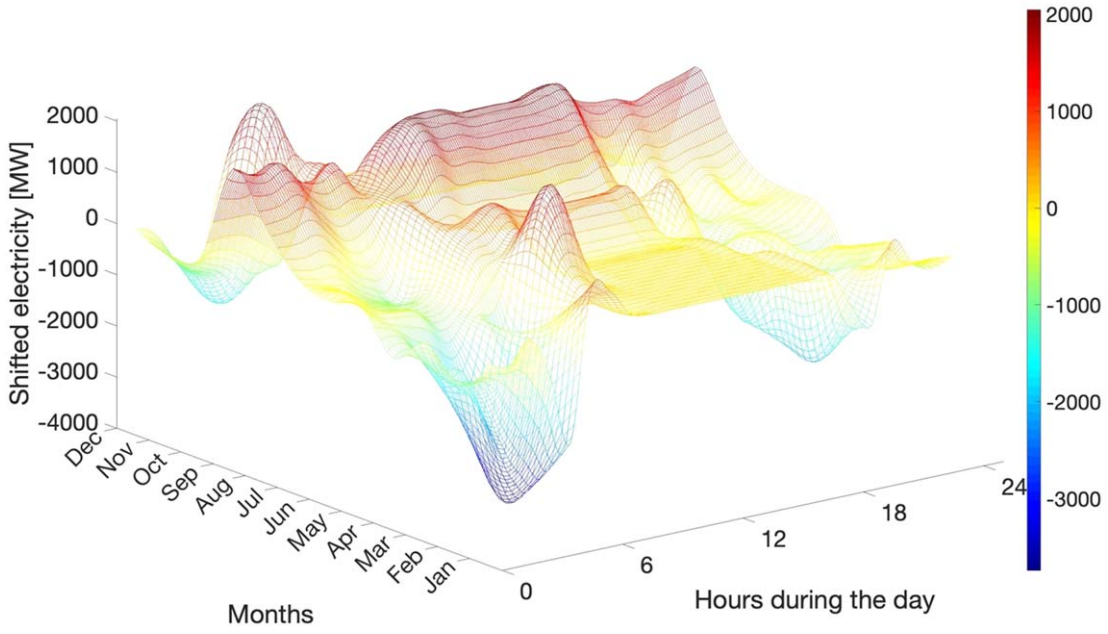

Figure 5. Average shifted load by month and daytime for the 10 d load-shifting period.

Table 1. Optimised electricity supply system after load-shifting with a 10 d period.

Fuel type	Capacity (GW)	Capacity share	Generation (TWh)	Generation share	Spillage (TWh)	Capacity factor
Hydro	3.7	2.7%	23.0	7.1%	0	71.1%
Biofuels	1.6	1.2%	5.0	1.5%	0	35.4%
Wind	42.7	31.7%	135.0	41.8%	13.4	39.7%
Utility PV	70.1	52.0%	119.1	36.9%	49.5	27.5%
CSP	12.3	9.1%	26.9	8.3%	9.5	33.8%
Ocean	0.21	0.2%	1.5	0.5%	0	83.6%
Geothermal	0.1	0.1%	0.7	0.2%	0	80.3%
Rooftop PV	4	3.0%	11.7	3.6%	0	33.5%
Total	135	100%	**322.9**	100%	**72.3**	**33.5%**

shifting are higher than the positive peaks. This effect stems from the limitation of maximum demand by caps. At the same time, this shows that the use of higher permissible demand could have a positive effect on the electricity system. In conclusion, we find that the ability to move demand both seasonally and across the hours of the day is useful for optimising the energy system.

3.2. Electricity supply-side and cost-implications

Table 1 provides an overview of the electricity supply resulting from load-shifting with a period of 10 d. Here, the total electricity generation capacity is 135 GW. We see that utility PV holds the highest share with 70.1 GW of generation capacity, which equates to 52% of the total capacity. The energy generated by utility PV (and utilised by the demand i.e. which is not spilt) is 119.1 TWh, which is only 36.9%. Wind energy has the largest share here, with 135.0 TWh and a share of 41.8%—the higher value for generated energy results from the fact that wind energy is the most continuous, compared to other volatile energy carriers. Therefore, wind energy can also achieve the relatively high capacity factor of 39.7%. Although energy sources with continuous availability such as ocean power have a very high capacity factor of up to 83.6%, they have minimal expansion potential.

Furthermore, wind energy, which contributes the largest share to the amount of electricity generated, has a relatively small amount of spilt energy itself. Only 13.4 TWh of the produced wind energy is lost. By way of comparison, utility PV generates 49.5 TWh of spilt energy. Thus, not even 9% of electricity produced by wind is spilt energy, whereas utility PV reaches 29%; The high value of the spilt PV energy, which is still prevalent even after the load-shifting, illustrates the range of PV electricity availability. High electricity supply with low demand prevails in many periods. Wind energy, on the other hand, is much more congruent with demand. If a load-shifting is performed, the spilt energy can thus be reduced by at least 27 TWh. If we increase the load-shifting period to 30 d and 90 d, the necessary generation capacity decreases to 122.5 GW and 114.5 GW respectively. Overall, desalination load-

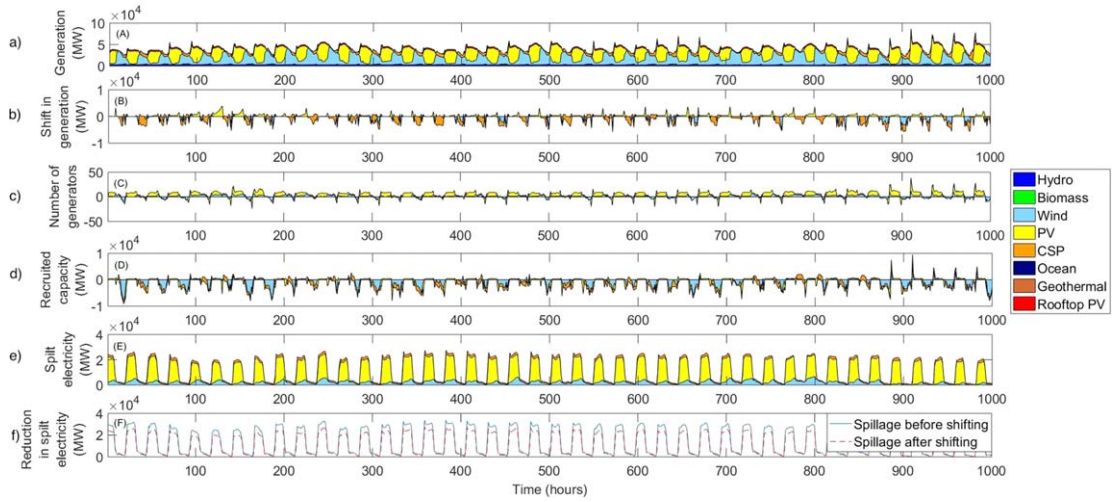

Figure 6. Electricity supply after the load-shifting process for a 10 d load-shifting period. With (a) generation, (b) shifted electricity, (c) number of shifted generators, (d) change in recruited capacity, (e) spilt electricity, (f) reduction in spilt electricity.

shifting can reduce the installed capacity and levelised cost of electricity (LCOE) by up to 29%, and 43%, respectively (see supplementary material S3 and S4 for further details).

Figure 6 presents the change in the electricity supply after load-shifting for a range of 1000 h. Subfigure (a) shows the structure of electricity generation. Utility PV is dominant among the generators. During the nights, wind power produces electricity, whereas during the days, utility PV dominates electricity production. Subfigure (b) shows the shifted generation. Positive values mean that electricity demand is shifted to the respective hour. Negative values indicate hours where electricity is no longer utilised. We can see that the load-shifting program has systematically replaced CSP and partially replaced wind with cheaper utility PV.

Subfigure (c) shows the change in the number of generators dispatched for electricity production after the load-shifting process. Subfigure (d) illustrates the recruited capacity of these generators. A negative recruited capacity means that the capacity utilised before the load-shifting is no longer needed at this hour. The program shifted the respective loads from more expensive to less expensive generators. At the end of an optimisation run, unused expensive generators are removed from the network.

Subfigures (e) and (f) visualise the spilt electricity. Figure (e) shows that a significant proportion of the spilt electricity comes from utility PV. Wind power, on the other hand, has a much smaller amount of spilt electricity. Now it becomes clear that on the one hand, the load-shifting program replaces wind power with PV; on the other hand, it shifts the demand so as to utilise more PV to reduce the total cost of the system. Figure (f) shows how the load-shifting optimises the generation structure. Hence, the peaks of spilt energy were reduced significantly. The results show that wind and solar complement each other under Australian conditions. The peaks of PV occur during the day, while the peaks of wind occur mostly at night. The use of CSP can further flatten the supply by the use of heat storages. Therefore, we recommend a mixed application of these technologies when combining with desalination.

3.3. Estimation of additional costs and benefits[8]

In the following, we estimated the benefits and costs directly related to the load-shifting. When load-shifting is applied, less power generation capacity is needed compared to the situation where no load-shifting would be applied. Hence, we define the additional benefit as saving in the total cost of electricity generation. We define the direct costs related to the load-shifting by the necessary increase in the desalination capacity. Our approach is a simple static analysis. Hence, we do not consider dynamic price changes or indirect effects, such as social effects. We provide further details on the assumptions and the calculation in the supplementary material S5. With applied load-shifting, the LCOE of power generation was 11.3–13.5 ct $kW^{-1}\,h^{-1}$. Without load-shifting, LCOE was 20 ct $kW^{-1}\,h^{-1}$. With the LCOEs and the respective total electricity quantities, we calculated the total costs of electricity generation for both the load-shifting scenarios and the basic scenario without load-shifting. The difference between the total costs of electricity results in an average gross economic benefit of $24.6 bn per year. This cost saving is made possible by not operating desalination plants continuously but providing their demand flexibly for load-shifting purposes. In our study, we applied an oversize factor of 1.5; in other words, the desalination and pipeline capacity were 50% higher than in a baseload scenario

[8] Explanations of the methodology and assumptions can be found in the supplementary material at S5.

for continuous operation throughout the year. To calculate the additional costs of the desalination plants and the pipelines, we used specific capital costs from IAEA (2013) and Bluefield Research (2018), respectively. Oversizing desalination plants results in an additional annuity of $1.27 bn. The expansion of pipeline capacity leads to an additional annuity of $809 m. In conclusion, considering desalination demand for load-shifting under the given assumptions promises high net economic benefits of $22.5 bn, which is 35% of the total cost of electricity in the no-shifting scenario.

3.4. Challenges and global prospects

Recently, we see a growing awareness of climate change worldwide. Movements, such as the protests movement of 'Fridays for Future', are pushing governments to take more determined action. The electricity sector plays a key role for a climate-neutral economy (Wolfram *et al* 2016), but a high proportion of RE in the electricity sector requires a fundamentally different network operation (Olatomiwa *et al* 2016). The slow implementation of RE technologies in Australia, although with very high meteorological potential, is a major obstacle to implementing these strategies. The slow adaptation, as well as the historically high dependence on coal, currently lead to a carbon lock-in of the Australian economy (Unruh 2000).

When implementing seawater desalination on this scale, other environmental effects must be considered. The impacts of brine discharge on the marine environment continue to be the subject of controversial research discussions (Darwish *et al* 2013) (Zhou *et al* 2014) (Mannan *et al* 2019) (Saeed *et al* 2019). However, in a recent large-scale ecological impact study, Clark *et al* (2018) have demonstrated that the effects of brine in seawater desalination are significantly smaller than previously thought. Furthermore, Seawater desalination is still costly, but the cost of technology has decreased significantly in recent decades. New research in the field of graphene for desalination shows that the energy efficiency of seawater desalination could once again decrease by a factor of more than 10 (Aghigh *et al* 2015). Through international agreements such as the Paris Agreement, countries worldwide will increasingly implement climate policy measures, whereby RE will become competitive by pricing CO_2.

In our study, we demonstrated the advantages of the combination of desalination plants, pipelines and RE. The calculated 35 pipelines with an average diameter of 2.1 m are an enormous challenge to build. Twenty-four locations can be supplied with just one pipeline each, two locations require two pipelines each, and one location requires three pipelines. An adaptation of the operational management, e.g. by pursuing a more continuous operation, would provide opportunities to reduce the number of pipelines at individual sites. We are aware of the magnitude of the idea of building seawater desalination plants with a capacity of 5500 Gl per year for the MDB. Cutting edge practice and research worldwide show that projects on this scale are a realistic option in the battle against drought: The Israeli government plans to save the drought-threatened Sea of Galilee with seawater desalination (The Economist 2018). To do this, they want to increase their desalination capacity and pump water from the Mediterranean Sea to the Sea of Galilee. At the World Water Conference 2019, the idea of a 'climate correction project' was presented (Stiftung Forschung für Leben 2019). The idea applies seawater desalination with RE to keep the rising sea level constant in the context of climate change. At the same time, according to this idea, water should be pumped into dry regions to increase vegetation and simultaneously to counteract climate change.

4. Conclusion

Our study focusses on two global challenges: First, global areas of arid regions are growing due to climate change. Second, the majority of the world community has agreed on ambitious CO_2 reductions for the coming decades, which should limit global temperature increases to 1.5 °C. This study proposes a combined solution of seawater desalination with RE. For this, we modelled a desalination and pipeline system to provide water for the MDB. RE contribute to making desalination plants sustainable. At the same time, desalination serves as a variable load, which reduces the generation capacity of RE plants and therefore, the cost of the system. With our approach, the generation capacity of the electricity system can be reduced by more than 29%. We achieve net annual cost savings of more than $22.5 bn, which equates to 35% of the total cost of electricity in the no-shifting scenario. Desalination is particularly suitable for load-shifting, because storing water for a longer period is affordable and technically feasible.

Our study showed how available flexible loads in a 100% RE system can significantly reduce the installed capacity. We demonstrated how sun and wind energy complement each other when coupling with desalination. Instead of operating with only one energy source, a mix of both is preferable. Furthermore, loads are advantageous, which can be shifted both, within a day and between seasons. However, the policy needs to create regulatory frameworks that price the external costs of carbon emissions and water extraction and distribute the benefits of load-shifting to the shiftable loads, i.e. desalination and pipeline operators, creating incentives to provide the necessary variable loads. Given the continuing aridity, the MDBA should limit the water extraction in the short term (in the 5500 Gl range) to increase environmental flows. In the medium term, water prices for extracted water should be

increased (e.g. through taxes) in order to ensure sustainable water use. In the long term, the collected taxes can be used to expand RE, desalination plants and pipelines.

Nonetheless, our study is limited to investigating the immediate interaction of RE and desalination plants. Our study does not analyse environmental, economic and social factors or compile a comprehensive cost-benefit analysis. We also do not compare with alternative water supply options, such as wastewater reuse or reducing water consumption. Even though these options are essential for the entire Australian water supply, we show a solution that is able to provide large volumes of water in dry coastal regions. We will investigate social, environmental and economic factors in detail in further research.

Acknowledgments

We thank Professor Dr Frank Behrendt from the Department of Energy Engineering of the Technical University of Berlin for his continuous support. This work was financially supported the Friedrich Naumann Foundation for Freedom. We acknowledge support by the German Research Foundation and the Open Access Publication Fund of TU Berlin. Finally, we also thank the anonymous reviewers for the valuable comments, which have improved this study.

Data availability statement

The data that support the findings of this study are available from the corresponding author upon reasonable request.

References

Aghigh A, Alizadeh V, Wong H Y, Islam M S, Amin N and Zaman M 2015 Recent advances in utilization of graphene for filtration and desalination of water: a review *Desalination* **365** 389–97

Alhaj M and Al-Ghamdi S G 2019a Integrating concentrated solar power with seawater desalination technologies: a multi-regional environmental assessment *Environ. Res. Lett.* **14** 74014

Alhaj M and Al-Ghamdi S G 2019b Why is powering thermal desalination with concentrated solar power expensive? assessing economic feasibility and market commercialization barriers *Sol. Energy* **189** 480–90

Ali S M H, Lenzen M and Huang J 2018 Shifting air-conditioner load in residential buildings: benefits for low-carbon integrated power grids *IET Renew. Power Gener.* **12** 1314–23

Ali S M H, Lenzen M and Tyedmers E 2019 Optimizing 100%-renewable grids through shifting residential water-heater load *Int. J. Energy Res.* **43** 1479–93

Aquasure 2015 *Victorian Desalination Project Fact Sheet—Pipeline and Power Supply* (https://aquasure.com.au/pipeline-powerline)

Augsten E 2007 Desalination by means of wind and sun *Sun Wind Energy* (https://sunwindenergy.com/system/files/swe_0702_032-037_desalination.pdf)

Baten R and Stummeyer K 2013 How sustainable can desalination be? *Desalination Water Treat.* **51** 44–52

Bennett A 2011 Cost effective desalination: innovation continues to lower desalination costs *Filtr. Sep.* **48** 24–7

Bluefield Research 2018 *Relative Piping Costs* (Boston, MA) (https://wateronline.com/doc/water-and-wastewater-pipeline-infrastructure-opportunities-0001)

Bognar K, Pohl R and Behrendt F 2013 Seawater reverse osmosis (SWRO) as deferrable load in micro grids *Desalination Water Treat.* **51** 1190–9

Bureau of Meteorology 2019 Monthly Weather Review (http://bom.gov.au/climate/mwr/)

Clark G F, Knott N A, Miller B M, Kelaher B P, Coleman M A, Ushiama S and Johnston E L 2018 First large-scale ecological impact study of desalination outfall reveals trade-offs in effects of hypersalinity and hydrodynamics *Water Res.* **145** 757–68

Connell D and Grafton R Q 2011 Water reform in the Murray–Darling basin *Water Resour. Res.* **47** W00G03

Crimp S J, Stokes C J, Howden S M, Moore A D, Jacobs B, Brown P R, Ash A J, Kokic P and Leith P 2010 Managing Murray–Darling basin livestock systems in a variable and changing climate: challenges and opportunities *Rangel. J.* **32** 293–304

Darwish M, Hassabou A H and Shomar B 2013 Using seawater reverse osmosis (SWRO) desalting system for less environmental impacts in Qatar *Desalination* **309** 113–24

Desalination.biz 2017 Chile project envisions multiple mining clients for solar-powered SWRO *Desalination.biz* (https://desalination.biz/news/3/Chile-project-envisions-multiple-mining-clients-for-solar-powered-SWRO/8761/)

El Saliby I, Okour Y, Shon H K, Kandasamy J and Kim I S 2009 Desalination plants in Australia, review and facts *Desalination* **247** 1–14

Forghani A, Alexandra J and Donaldson J 2011 *Spatially Enabled MDBA* (Canberra) (http://csdila.unimelb.edu.au/BeyondSpatialEnablement/pdf/Forghani.pdf)

Freire-Gormaly M and Bilton A M 2018 Experimental quantification of the effect of intermittent operation on membrane performance of solar powered reverse osmosis desalination systems *Desalination* **435** 188–97

Ghaffour N, Lattemann S, Missimer T, Ng K C, Sinha S and Amy G 2014 Renewable energy-driven innovative energy-efficient desalination technologies *Appl. Energy* **136** 1155–65

Ghobeity A and Mitsos A 2010 Optimal time-dependent operation of seawater reverse osmosis *Desalination* **263** 76–88

Grubert E A and Webber M E 2015 Energy for water and water for energy on Maui Island, Hawaii *Environ. Res. Lett.* **10** 64009

Heihsel M, Lenzen M, Malik A and Geschke A 2019 The carbon footprint of desalination: an input–output analysis of seawater reverse osmosis desalination in Australia for 2005–2015 *Desalination* **454** 71–81

Hoekstra A Y, Chapagain A K, Aldaya M M and Mekonnen M M 2011 *The water footprint assessment manual—setting up the global standard* (London) (https://waterfootprint.org/media/downloads/TheWaterFootprintAssessmentManual_2.pdf)

Hoekstra A Y, Mekonnen M M, Chapagain A K, Mathews R E and Richter B D 2012 Global monthly water scarcity: blue water footprints versus blue water availability *PLoS One* **7** e32688

IAEA 2013 Desalination Economic Evaluation Program 5.1 (https://pub.iaea.org/MTCD/Publications/PDF/CMS-19_web.pdf)

Keck F, Lenzen M, Vassallo A and Li M 2019 The impact of battery energy storage for renewable energy power grids in Australia *Energy* **173** 647–57

Kirby M, Bark R, Connor J, Qureshi M E and Keyworth S 2014 Sustainable irrigation: How did irrigated agriculture in Australia's Murray–Darling basin adapt in the millennium drought? *Agric. Water Manag.* **145** 154–62

Kirby M, Connor J, Bark R, Qureshi E and Keyworth S 2012 The economic impact of water reductions during the Millennium Drought in the Murray-Darling Basin *56th AARES Annu. Conf. Fremantle, West. Aust. Febr. 56th AARES Annu. Conf.*

Fremantle (West. Aust., 7–10 February) (https://doi.org/10.22004/ag.econ.124490)
Leblanc M, Tweed S, Van Dijk A and Timbal B 2012 A review of historic and future hydrological changes in the Murray–Darling Basin *Glob. Planet. Change* **80–81** 226–46
Leck H, Conway D, Bradshaw M and Rees J 2015 Tracing the water-energy-food nexus: description *Theory Practice Geogr. Compass* **9** 445–60
Lenzen M, McBain B, Trainer T, Jütte S, Rey-Lescure O and Huang J 2016 Simulating low-carbon electricity supply for Australia *Appl. Energy* **179** 553–64
Li S, Cai Y-H, Schäfer A I and Richards B S 2019 Renewable energy powered membrane technology: a review of the reliability of photovoltaic-powered membrane system components for brackish water desalination *Appl. Energy* **253** 113524
Mannan M, Alhaj M, Mabrouk A N and Al-Ghamdi S G 2019 Examining the life-cycle environmental impacts of desalination: a case study in the State of Qatar *Desalination* **452** 238–46
Murray–Darling Basin Authority 2010 *Guide to the proposed Basin Plan: Technical background* (Canberra) (https://mdba.gov.au/sites/default/files/archived/guide_pbp/Guide-to-proposed-BP-vol2-0-12.pdf)
Murray–Darling Basin Authority 2018 Transition Period Water Take Report *2016–17. Report on Cap compliance and transitional SDL accounting* (https://mdba.gov.au/sites/default/files/pubs/transition-period-water-take-report-2016-17.pdf)
Murray–Darling Basin Authority 2019a Discover the Basin (https://mdba.gov.au/discover-basin)
Murray–Darling Basin Authority 2019b Murray–Darling Basin Government Storages (https://mdba.gov.au/managing-water/water-storage)
Murray–Darling Basin Authority 2012 *Basin Plan 2012* (Canberra: Australian Government) (https://www.legislation.gov.au/Details/F2017C00078)
Olatomiwa L, Mekhilef S, Ismail M S and Moghavvemi M 2016 Energy management strategies in hybrid renewable energy systems: a review *Renew. Sustain. Energy Rev.* **62** 821–35
Park G L, Schäfer A I and Richards B S 2011 Renewable energy powered membrane technology: the effect of wind speed fluctuations on the performance of a wind-powered membrane system for brackish water desalination *J. Membr. Sci.* **370** 34–44
Park G L, Schäfer A I and Richards B S 2012 The effect of intermittent operation on a wind-powered membrane system for brackish water desalination *Water Sci. Technol.* **65** 867–74
Porter M G, Downie D, Scarborough H, Sahin O and Stewart R A 2015 Drought and desalination: Melbourne water supply and development choices in the twenty-first century *Desalination Water Treat.* **55** 2278–95
Richards B S, Park G L, Pietzsch T and Schäfer A I 2014 Renewable energy powered membrane technology: Brackish water desalination system operated using real wind fluctuations and energy buffering *J. Membr. Sci.* **468** 224–32
Richards L A, Richards B S and Schäfer A I 2011 Renewable energy powered membrane technology: salt and inorganic contaminant removal by nanofiltration/reverse osmosis *J. Membr. Sci.* **369** 188–95
Richter B D, Davis M M, Apse C and Konrad C 2012 A presumptive standard for environmental flow protection *River Res. Appl.* **28** 1312–21
Saeed M O, Ershath M M and Al-Tisan I A 2019 Perspective on desalination discharges and coastal environments of the Arabian Peninsula *Mar. Environ. Res.* **145** 1–10
Scanlon B R, Duncan I and Reedy R C 2013 Drought and the water-energy nexus in texas *Environ. Res. Lett.* **8** 45033
Shahzad M W, Burhan M, Ang L and Ng K C 2017 Energy-water-environment nexus underpinning future desalination sustainability *Desalination* **413** 52–64
Stiftung Forschung für Leben 2019 Climate Correction Project (http://climate-correction-project.com)
The Economist 2018 Can the Sea of Galilee be saved? *Econ* (https://economist.com/middle-east-and-africa/2018/12/01/can-the-sea-of-galilee-be-saved)
The Parliament of Australia 2007 *Water Act 2007* (Canberra: The Parliament of Australia) (https://www.legislation.gov.au/Details/C2017C00151)
The World Bank 2012 *Renewable energy desalination. An emerging solution to close the water gap in the Middle East and North Africa* (Washington, DC: World Bank) (http://documents.worldbank.org/curated/en/443161468275091537/Renewable-energy-desalination-an-emerging-solution-to-close-the-water-gap-in-the-Middle-East-and-North-Africa)
Unruh G C 2000 Understanding carbon lock-in *Energy Policy* **28** 817–30
Williams J and Grafton R Q 2019 Missing in action: possible effects of water recovery on stream and river flows in the Murray–Darling Basin, Australia *Australas. J. Water Resour.* (https://doi.org/10.1080/13241583.2019.1579965)
Wittwer G and Griffith M 2011 Modelling drought and recovery in the southern Murray–Darling basin *Aust. J. Agric. Resour. Econ.* **55** 342–59
Wolfram P, Wiedmann T and Diesendorf M 2016 Carbon footprint scenarios for renewable electricity in Australia *J. Clean. Prod.* **124** 236–45
Zhou J, Chang V W C and Fane A G 2014 Life cycle assessment for desalination: a review on methodology feasibility and reliability *Water Res.* **61** 210–23
Ziolkowska J R 2015 Is desalination affordable? regional cost and price analysis *Water Resour. Manag.* **29** 1385–97